

Published in final edited form as:

*Pediatr Radiol.* 2014 October ; 44(10): 1310–1317. doi:10.1007/s00247-014-2983-3.

## $\gamma$ -H2AX foci are increased in lymphocytes in vivo in young children 1 h after very low-dose X-irradiation: a pilot study

**Brunhild M. Halm,**

University of Hawaii Cancer Center, 1236 Lauhala St., Honolulu, HI 96813, USA

**Adrian A. Franke,**

University of Hawaii Cancer Center, 1236 Lauhala St., Honolulu, HI 96813, USA

**Jennifer F. Lai,**

University of Hawaii Cancer Center, 1236 Lauhala St., Honolulu, HI 96813, USA

**Helen C. Turner,**

Center for Radiological Research, Columbia University Medical Center, New York, NY 10032, USA

**David J. Brenner,**

Center for Radiological Research, Columbia University Medical Center, New York, NY 10032, USA

**Vatche M. Zohrabian,** and

Center for Radiological Research, Columbia University Medical Center, New York, NY 10032, USA

**Robert DiMauro**

Kapi'olani Medical Center for Women and Children, Honolulu, HI 96826, USA

Brunhild M. Halm: hildahalm@earthlink.net

### Abstract

**Background**—Computed tomography (CT) is an imaging modality involving ionizing radiation. The presence of  $\gamma$ -H2AX foci after low to moderate ionizing radiation exposure has been demonstrated; however it is unknown whether very low ionizing radiation exposure doses from CT exams can induce  $\gamma$ -H2AX formation in vivo in young children.

**Objective**—To test whether very low ionizing radiation doses from CT exams can induce lymphocytic  $\gamma$ -H2AX foci (phosphorylated histones used as a marker of DNA damage) formation in vivo in young children.

**Materials and methods**—Parents of participating children signed a consent form. Blood samples from three children (ages 3–21 months) undergoing CT exams involving very low blood ionizing radiation exposure doses (blood doses of 0.22–1.22 mGy) were collected immediately

before and 1 h post CT exams. Isolated lymphocytes were quantified for  $\gamma$ -H2AX foci by a technician blinded to the radiation status and dose of the patients. Paired *t*-tests and regression analyses were performed with significance levels set at  $P < 0.05$ .

**Results**—We observed a dose-dependent increase in  $\gamma$ -H2AX foci post-CT exams ( $P = 0.046$ ) among the three children. Ionizing radiation exposure doses led to a linear increase of foci per cell in post-CT samples (102% between lowest and highest dose).

**Conclusion**—We found a significant induction of  $\gamma$ -H2AX foci in lymphocytes from post-CT samples of three very young children. When possible, CT exams should be limited or avoided by possibly applying non-ionizing radiation exposure techniques such as US or MRI.

### Keywords

Children; Radiation dose; Lymphocytic  $\gamma$ -H2AX foci formation; Computed tomography

---

### Introduction

Computed tomography (CT) is an essential imaging modality of modern medicine that has revolutionized the diagnosis of traumatic injuries and a variety of conditions such as headache, seizures, complicated pneumonias and abdominal pain [1, 2].

CT use has increased substantially during the last few decades [3], particularly for children presenting to an emergency department [2, 3]. Although the rise of CT use has lessened in the last few years [4, 5], the frequency of pediatric CT exams is still very high, and this raises special concerns about the long-term risks associated with diagnostic ionizing radiation exposure.

Ionizing radiation exposure is a risk factor for cancer in humans [6]. Ionizing radiation exposure can induce DNA double-strand breaks (the most deleterious genetic lesions), which, in turn, can trigger several detrimental cellular responses including carcinogenesis [7]. Ionizing radiation exposure from diagnostic exams such as CT scans has been estimated to contribute to 1.5–2.0% of all cancers in the United States [3], with cancer risk being highest for very young children [8] because of their enhanced radiosensitivity and longer life expectancy compared to adults [9–11]. These estimations are based on the linear-no-threshold model, which extrapolates cancer risks from dose–response data from populations exposed to short-term/acute radiation doses ranging up to 0.2 Gy, 0.5 Gy, 1 Gy or higher [12] to lower chronic ionizing radiation exposure dose ranges of 100 mGy or less or dose rates lower than 6mGy per hour (when averaged over the first few hours) [12, 13] on the assumption that cellular effects such as DNA damage occur in direct proportion to ionizing radiation exposure at all levels, thereby implying that no threshold level can be considered risk-free [14, 15].

This extrapolation, however, has been debated among the scientific community and questioned by some authors [16, 17], who argue that no negative radiation effects exist in the low ionizing radiation exposure dose range and that there might even be a hormetic effect.

For clarification, the terms defining relative levels of ionizing radiation exposure (e.g., “moderate to high dose radiation exposure,” “lower ionizing radiation exposure dose ranges,” and “the low ionizing radiation exposure dose range”) have not been adequately and/or definitively defined in published literature. However, for the purpose of quantifying cancer risk associated with radiation exposure the ICRP used as a rule of thumb, effective doses relating to 1 Sv, 100 mSv, 10 mSv, 1 mSv, and 0.1 mSv to signify the terms “moderately high,” “moderate,” “low,” “very low,” and “extremely low” doses, respectively [12]. On the other hand, among literature data, these definitions have varied. For example, Feinendegen [17] defined low-dose radiation less than 200 mGy and a review by Brenner and Hall [3] reported low-dose radiation to be between 5 and 150 mSv while Brenner et al. [18] stated intermediate and high doses of ionizing radiation as more than 100 mSv.

One realistic definition of “low dose of radiation,” as suggested by ICRP, is a threshold below which it remains impossible to detect radiation-related adverse health effects; thus, alternatively, the suggested level of 20 rads, 20,000 mrad, or 0.2 Gy, 200 mGy is another threshold that could be used to define low-dose radiation.

Two recently published retrospective studies looked at the development of cancer in children and adolescents with a history of low-dose ionizing radiation exposure. Relative risk of leukemia was reported to approximately triple in children younger than 15 years of age after receiving 5–10 head CT scans equivalent to organ dose (approximately 50 mGy to red bone marrow) [19]. Relative risk of brain cancer was reported to approximately triple in children younger than 15 years of age after receiving 2–3 head CT scans equivalent to organ dose (approximately 60 mGy to brain) [19]. Effective doses were not given [19]. More disturbingly, the study found that the long-term effects of childhood ionizing radiation exposure may not become apparent until after several decades [19]. Compared to non-exposed individuals Mathews et al. [20] found a greater incidence (24%) for all cancer types when children or adolescents were exposed to radiation from CT scans (the average radiation effective dose per scan was estimated at 4.5 mSv) with a dose-dependent increase in incidence risk rate of 16% per scan.

For brain cancers and all other cancers combined, the incidence rate ratios were highest for very young children and increased with the number of CT scans [19, 20].

One of the most frequently used biomarkers for the biological effects of ionizing radiation exposure is gamma-H2AX ( $\gamma$ -H2AX) foci, clusters of the phosphorylated form of the core histone variant H2AX. These foci are formed rapidly (within 3 min) after ionizing radiation exposure as a cellular response, specifically at sites of DNA double-strand breaks [21–24], with one focus indicating one DNA double-strand break. Gamma-H2AX foci formation has been shown to precede the assembly of DNA-repair complexes and has thus been deemed essential for DNA damage repair [25].

Lymphocytic  $\gamma$ -H2AX foci can be visualized using an immunofluorescence-based microscopy assay [23, 26, 27], and several studies have demonstrated the sensitivity of  $\gamma$ -H2AX foci detection. Redon and colleagues [28] found linear increases in lymphocytic  $\gamma$ -H2AX foci per cell from rhesus macaques irradiated in vivo using total body irradiation

doses of  $^{60}\text{Co}$ - $\gamma$ -rays ranging from 1 Gy to 8.5 Gy. Adults undergoing CT scans of the thorax or abdomen showed a dose-dependent increase in lymphocytic foci 30 min after ionizing radiation exposure [27], while children undergoing cardiac catheterization with concomitant fluoroscopic X-ray exposure (median effective dose of 6.4 mSv) showed a dose-dependent increase in  $\gamma$ -H2AX foci per cell [29]. Linear increases in  $\gamma$ -H2AX foci from healthy human lymphocytes irradiated *ex vivo* with 0–8 Gy of  $\gamma$ -rays [26] and 0.2–5 Gy [30] have also been observed. Although these studies demonstrate the sensitivity of  $\gamma$ -H2AX foci detection after low to high ionizing radiation exposure in humans *in vivo*, it is unknown whether very low ionizing radiation doses from CT exams would also change  $\gamma$ -H2AX formation *in vivo* in very young children. Therefore, the aim of this pilot study was to elucidate whether very low ionizing radiation exposure doses from medically indicated CT scans in very young children would result in changes in  $\gamma$ -H2AX foci formation.

## Materials and methods

### Patients

This HIPAA-compliant study was approved by the associated institutional review boards and was performed in accordance with the ethical standards laid down in the 1964 Declaration of Helsinki and its amendments. Three boys (3–21 months old) undergoing medically indicated CT scans in the emergency department at Kapi'olani Medical Center for Women and Children in Honolulu, Hawaii participated in this study after their parents signed a consent form. Exclusion criteria included children with immediate risk of decompensation, children weighing less than 9 lbs, and children with complex medical problems such as cancer. Contact information for parents or legal guardians of participating children were obtained along with questions regarding the child's age, birth history, medical history, medication use, ethnicity, overall health condition, allergies, height and weight and vitamin intake. In all patients, a detailed radiologic history was collected from the interview with the parents and also through hospital records. Blood draws and CT scan times were documented, as were dose-length products (in mGy-cm).

### Radiation

CT examinations were performed using a GE LightSpeed VCT Select 64-slice CT scanner (GE Healthcare, Waukesha, WI) operated at 199–300 mA and 100–120 kVp with a 0.4–0.5 exposure time per rotation. The collimation (beam width) was 20 mm and the pitch varied from 1.00 to 1.38. These parameters provided volumetric CT dose indices (CTDI vol in mGy) for a 16-cm phantom of 6.40 to 21.31. The dose-length products, calculated as the sum of the products of the CTDI vol multiplied by the scan length for each phase, ranged from 92.46 mGy-cm to 426.12 mGy-cm. The effective doses ranged from 1.57 mSv to 2.86 mSv.

Because dose-length product is the dose received by a 16-cm diameter CTDI phantom (not patient) and poorly represents patient organ or tissue dose, we calculated blood or lymphocyte dose, which is more relevant than dose-length product when looking at changes in blood from ionizing radiation exposure.

Ionizing radiation exposure from medical imaging procedures is commonly and quantitatively compared in terms of effective dose (in units of Sieverts, Sv) to account for every equivalent dose received by all the tissues and organs of the body. However, because the radiosensitivity of all organs is not universal, the use of the effective dose provides, at best, only an approximately proportional estimate of the overall insult to a patient receiving ionizing radiation exposure [3]. For this reason, in our study we were interested in obtaining the blood dose calculations.

### Calculation of the organ and blood doses

We calculated organ doses using the software CT-Expo version 1.7 (Medizinische Hochschule, Hannover, Germany), and the options “baby” and “child” were selected depending on the child’s age [31]. In addition to the organ dose, the individual blood doses were calculated. Because of the different distribution of blood throughout the body, we weighted the calculated organ doses by the fraction of the total blood volume present in each of these organs at any given time, according to values present in the ICRP publication 89 [32]; these values were then summed and resulted in mean blood doses of 0.22 mGy, 1.22 mGy, and 0.77 mGy for patients 1, 2 and 3, respectively (Table 1).

### Sample collection and processing

Peripheral heparinized whole blood (2 ml) was collected by venipuncture from each child immediately before and 1 h after their scheduled CT exams. When possible, EMLA cream (Astrazenica, Wilmington, DE) was used to minimize pain during venipuncture. If a normal saline IV lock was in place for medical reasons, 2.5ml of blood was first withdrawn and discarded before collecting the blood for the study. After the CT scan, both pre- and post-CT tubes were immediately transferred to the University of Hawaii Cancer Center laboratory at room temperature and protected from light.

### Lymphocyte isolation from whole blood

Immediately upon arrival in the laboratory, lymphocytes were isolated from whole blood by adding 3 ml of separation media (Histopaque<sup>®</sup>-1077; Sigma-Aldrich, St. Louis, MO) to the upper chamber of Accuspin<sup>™</sup> tubes (Sigma-Aldrich, St. Louis, MO) followed by centrifugation at  $800 \times g$  for 30 s. Three milliliters of whole blood were then poured into the upper chamber of each tube and centrifuged at  $800 \times g$  for 15 min. Whole blood was diluted with Gibco<sup>®</sup> RPMI medium (Invitrogen, Eugene, OR) to make up the volume to 3 ml. After centrifugation, the plasma layer was discarded and lymphocytes were recovered from the interface between the plasma and separation media. Lymphocytes were transferred to a 15-ml conical tube and washed three times with 5–10 ml phosphate buffered saline (PBS). Each wash consisted of PBS addition, gentle resuspension by air mixing with a Pasteur pipette, and centrifugation at  $250 \times g$  for 10 min. After the third wash, the PBS supernatant was removed and a fresh 500  $\mu$ l volume of PBS was added to re-suspend the cells. The re-suspended lymphocytes were fixed in 6–8 ml of ice-cold methanol and kept at 8°C until analysis. An aliquot of fixed lymphocytes was visually checked under the microscope for membrane integrity by a histotechnologist at the University of Hawaii Cancer Center.

## $\gamma$ -H2AX detection in lymphocytes

The methanol-fixed samples were de-identified prior to shipment to the Center for High-Throughput Minimally Invasive Radiation Biodosimetry, Columbia University Medical Center (New York, NY), in order to blind the  $\gamma$ -H2AX detection regarding CT status and radiation dose. Samples were shipped on wet ice and stored at 8°C upon arrival. Prior to use, all samples were centrifuged at  $213 \times g$  for 10 min to form pellets of the fixed cells followed by removal of the methanol supernatant and re-suspension in approximately 500  $\mu$ l of fresh methanol. For immunodetection of the  $\gamma$ -H2AX protein, the cells were blocked with 3% bovine serum albumin for 30 min and incubated with an anti-human  $\gamma$ -H2AX monoclonal antibody (dilution 1:750, ab18311; Abcam Inc., Cambridge, MA) for 1 h at room temperature. Following three 10-min washes with PBS the cells were exposed to Alexa Fluor 488 (AF488) secondary antibody (dilution 1:1,000; Invitrogen, Eugene, OR) for 50 min. The cells were again thrice washed for 10 min in PBS and then counterstained and mounted with Vectashield Mounting Medium with DAPI (H-1200; Vector Laboratories, Burlingame, CA) and sealed with a coverslip. The samples were visualized using an Olympus epifluorescent microscope (Olympus BX43F; Center Valley, PA). The number of  $\gamma$ -H2AX foci per nucleus for all samples was counted manually. Immunostaining was performed in duplicate for both pre- and post-CT samples in a blinded fashion.  $\gamma$ -H2AX foci enumeration (per cell) was performed for each pre- and post-CT replicate and the averages foci/cell counts were used for comparison.

More than 100 cells were manually counted per participant, with more than 60 cells being counted for each pre- and postionizing radiation exposure duplicate.

## Statistical methods

Student's paired *t*-tests for significance and regression analyses were performed with Excel (Microsoft, Seattle, WA). A *P*-value of  $<0.05$  was considered statistically significant.

## Results

Demographic characteristics of the participants are shown in Table 2. Pre-CT  $\gamma$ -H2AX foci values among the patients were similar (range  $1.26 \pm 0.16$ – $1.53 \pm 0.42$  foci per cell) but increased for all three patients 1 h after CT scans ( $P=0.046$  by paired *t*-tests). Mean ionizing radiation exposure blood doses of 0.22–1.22 mGy led to mean  $\pm$  SD pre–post CT increases of  $0.96 \pm 0.13$  (Patient 1),  $1.16 \pm 0.30$  (Patient 3) and  $1.95 \pm 0.09$  (Patient 2) foci per cell, respectively (Fig. 1), on average a doubling (102%) of foci per cell between the lowest and highest ionizing radiation exposure dose. This increase in foci per cell was linearly dependent on dose-length product dose ( $P=0.002$  by regression analysis). Replicate blinded  $\gamma$ -H2AX foci counting from separate lymphocyte aliquots showed a mean inter-assay coefficient of variations of 11% (four separate assays for each patient). Post-CT duplicates showed a lower coefficient of variations than pre-CT duplicates (4% vs. 17%) probably because of the easier-to-read higher absolute values of the former. Pre- and post-CT  $\gamma$ -H2AX for patient 3 are shown in Fig. 2.

## Discussion

We observed in vivo the formation of  $\gamma$ -H2AX foci in peripheral blood lymphocytes from young children who underwent CT exams for medical reasons. Our results indicate that  $\gamma$ -H2AX is a reliable and sensitive biomarker to evaluate the effects of very low-dose ionizing radiation exposure—with a mean coefficient of variation of only 11% for our blinded replicates. Although our sample size was very small ( $n=3$ ), we observed a linear increase in  $\gamma$ -H2AX foci post-CT, depending on dose-length product, even at effective doses as low as 1.57 mSv (blood dose of 0.22 mGy). We also observed a dose response relationship between  $\gamma$ -H2AX foci and radiation dose, which implies a causal role of CT for the observed changes. However, it is possible that chance alone could explain the results.

We emphasize that our results are very preliminary and advise caution on over-drawing definitive, wide-reaching conclusions. Control subjects were not included in this preliminary pilot study as to minimize participant burden. However, with the knowledge gained from this study we can now design larger studies (with very low blood ionizing radiation exposure doses equal to those in our study) that will include control groups in order to confirm our findings. Alternatively, studies using other tests for detecting chromosome abnormalities, such as the cytokinesis-block micronucleus assay (currently the most widely used assay to quantify lymphocytic micronucleus frequency [33]) might also be used to verify the presence of  $\gamma$ -H2AX foci. Chromosomal aberrations and micronuclei in peripheral blood lymphocytes after ionizing radiation exposure are validated biomarkers of somatic chromosomal damage and constitute the clinically relevant endpoints in carcinogenesis [34, 35]. However, the sensitivity of these cytogenetic techniques might not be sufficient for individual biological dosimetry of patients receiving ionizing radiation doses less than 50 mSv, as in our study [36, 37].

The ionizing radiation doses applied in our study are lower than other studies measuring  $\gamma$ -H2AX foci after CT exams. Löbrich et al. [27] investigated ionizing radiation exposure-induced lymphocytic  $\gamma$ -H2AX foci formation in vivo in adults undergoing CT exams and in vitro using irradiated human fibroblasts. In vivo induction of  $\gamma$ -H2AX foci by CT was found to increase dose dependently to the dose-length product for values as low as 150 mGy-cm, corresponding to an estimated blood dose of approximately 3 mGy. More recently, Beels et al. [38] found a linear biphasic response of foci formation relative to blood dose. However, the lowest blood dose used in that study was 2.1 mGy and the population consisted exclusively of adults [38]. In our study effective doses ranged from 1.57 mSv to 2.86 mSv, corresponding to blood doses ranging from 0.22 mGy to 1.22 mGy.

Blood dose calculations were performed by weighting the organ-specific doses (derived from CT-Expo; see Materials and methods) against the fraction of total blood volume present in the respective organs using regional blood volumes from the ICRP Publication 89 [21–23, 32]. The individual weighted organ doses were then summed. Although this blood dose calculation method has been used in adults [37], there is some uncertainty in our estimations with children because the blood volumes used for calculation were derived from adult populations. Also, depending on the physiological state of a child, the amount of regional/local blood flow and blood volume can vary greatly and we cannot always assume

the average perfusion rate taken from a population sample is representative of the actual perfusion rate in a specific patient at a specific time. For example, children with a fever or in a state of inflammation (as in two of our patients) have increased blood flow at the site of inflammation. Consequently, there is an increased amount of blood exposed to radiation if significant inflammation is occurring at the area being scanned, in which case the amount of blood exposed to radiation during the CT scan is increased, which can systemically bias the results.

It is also noteworthy that the dose estimates used for calculating blood doses of our participants are generic in that they are derived from the CT-Expo software [31], which provides CT-scanner-specific dose estimates for a 2-month-old baby with a height of 57 cm and weight of 4.2 kg, and a 7-year-old child with a height of 115 cm and weight of 21.7 kg [39]. The CT-Expo dose estimates are based on calculated scanner-specific dose conversion coefficients from measured scanner-specific quantities to dose, and the combined systematic and random uncertainties of the dose conversion coefficients used are  $\pm 10\%$  [40]. The dose estimates used in the current work were based on those for the 2-month-old baby, which is younger than the subjects in the current study (3–21 months). Comparing CT-Expo dose estimates for the baby and the child, this could result in an underestimate of the actual patient doses by as much as 20%.

The regional blood volumes in infants and children are different from those in adults because of physiological and anatomical differences, and we are unaware of any systematic data on regional blood volume estimations in the pediatric population. However, human studies have demonstrated that cardiac output to kidneys is substantially lower in infants than in adults but gradually increases with age up to 3 years [32], while animal studies have indicated that blood perfusion rates and skeleton blood content may be 2–3 times higher in younger versus mature adults [32].

In the present study, blood samples were collected 1 h after CT exams. A previous study that also collected blood samples 1 h post-CT found that  $\gamma$ -H2AX foci yield was only 70% of that from samples taken 30 min post-CT, a foci loss thought to correspond to double-strand break repair [24]. The foci loss seemed to be dose-dependent and was noted up to 24 h, at which time the background level was reached [27]. Results from that study suggest that we could have detected more foci in our samples had the blood been drawn 30 min post-CT or perhaps repeatedly over the course of several hours, a key limitation in our study. However, because of the young age of the patients and circumstances under which the patients were admitted, we found it both inappropriate and a burden to repeatedly assess the patients over time. Additionally, repeated assessment would have been especially challenging because two of the three children were discharged home from the emergency department and follow-up would have been too difficult.

The repair kinetics of  $\gamma$ -H2AX foci are complex and depend on many factors. It has been suggested that contrast material commonly used for CT influences lymphocytic  $\gamma$ -H2AX foci formation. Although one of our patients required intravenous contrast administration prior to his CT scan, several studies have shown no relevant change in the number of  $\gamma$ -H2AX foci in the diagnostic dose range for both radiation and contrast agent dose [41].



## Conclusion

The results of our pilot study support the linear-no-threshold hypothesis [14, 15] at very low doses in young children. Our data suggest that even very low ionizing radiation exposure relevant to diagnostic CT exposure can leave a mark in the somatic DNA. When CT is necessary, great care should be taken to optimize radiation exposure to reduce radiation burden. The dose settings of the CT scanners should be kept as low as reasonably achievable while maintaining an image quality good enough for an accurate diagnosis [42]. Children exposed to a significant amount of ionizing radiation exposure for medical reasons are part of a large and growing population. Although radiologic procedures involve a small risk, this risk must be balanced against the potential benefits, especially when multiple procedures are to be performed during an individual's lifetime. Unnecessary radiation-producing procedures should be eliminated when possible and, if appropriate, non-ionizing techniques such as US or MRI should be used [38, 43, 44].

## Acknowledgments

We wish to thank the children and their parents who participated in the study. We would also like to thank Mr. Ronald Frick, MS, from the Gamma Corp. for his assistance in the CT parameters and calculations and Lynn Wilkens, PhD, for her statistical evaluation assistance. This study was funded by the University of Hawai'i Cancer Center Developmental Fund and the National Institute of Allergy and Infectious Diseases U19 AI067773 with the two senior authors (B.M.H and A.A.F.) as co-principal investigators and both contributing equally to this manuscript.

## References

1. Frush DP, Donnelly LF. Helical CT in children: technical considerations and body applications. *Radiology*. 1998; 209:37–48. [PubMed: 9769810]
2. Larson DB, Johnson LW, Schnell BM, et al. Rising use of CT in child visits to the emergency department in the United States, 1995–2008. *Radiology*. 2011; 259:793–801. [PubMed: 21467249]
3. Brenner DJ, Hall EJ. Computed tomography—an increasing source of radiation exposure. *N Engl J Med*. 2007; 357:2277–2284. [PubMed: 18046031]
4. Menoch MJ, Hirsh DA, Khan NS, et al. Trends in computed tomography utilization in the pediatric emergency department. *Pediatrics*. 2012; 129:e690–e697. [PubMed: 22331345]
5. Growth rate of U.S. CT scans is slowing. *Health Devices*. 2012; 41:332–333. No authors listed. [PubMed: 23444675]
6. Hsu WL, Preston DL, Soda M, et al. The incidence of leukemia, lymphoma and multiple myeloma among atomic bomb survivors: 1950–2001. *Radiat Res*. 2013; 179:361–382. [PubMed: 23398354]
7. Su TT. Cellular responses to DNA damage: one signal, multiple choices. *Annu Rev Genet*. 2006; 40:187–208. [PubMed: 16805666]
8. Berrington de Gonzalez A, Mahesh M, Kim K-P, et al. Projected cancer risks from computed tomographic scans performed in the United States in the 2007. *Arch Intern Med*. 2009; 169:2071–2077. [PubMed: 20008689]
9. Cardis E, Vrijheid M, Blettner M, et al. The 15-country collaborative study of cancer risk among radiation workers in the nuclear industry: estimates of radiation-related cancer risks. *Radiat Res*. 2007; 167:396–416. [PubMed: 17388693]
10. Berrington de Gonzalez A, Darby S. Risk of cancer from diagnostic X-rays: estimates for the UK and 14 other countries. *Lancet*. 2004; 363:345–351. [PubMed: 15070562]
11. Brenner D, Elliston C, Hall E, et al. Estimated risks of radiation-induced fatal cancer from pediatric CT. *AJR Am J Roentgenol*. 2001; 176:289–296. [PubMed: 11159059]
12. ICRP. Low-dose extrapolation of Radiation-related cancer risk. 2005 ICRP Publication 99. *Ann ICRP* 35.

13. UNSCEAR. United Nations Scientific Committee on the effects of atomic radiation. In: Nations U. , editor. Sources, effects and risks of ionizing radiation. United Nations, New York: 1993.
14. IARC. Ionizing radiation, Part 1: X- and gamma-radiation and neutrons. IARC monographs on the evaluation of carcinogenic risks to humans. Lyon: National Research Council, Committee on the Biological Effects of Ionizing Radiation, Health Risks from Exposures to Low Levels of Ionizing Radiation (BEIR VII); 2000.
15. UNSCEAR. United Nations Scientific Committee on the Effects of Atomic Radiation: sources, effects and risks of ionizing radiation. In: Publications UN. , editor. Scientific Annex B: Effects of radiation exposure of children. New York: 2013.
16. Tubiana M, Feinendegen LE, Yang C, et al. The linear no-threshold relationship is inconsistent with radiation biologic and experimental data. *Radiology*. 2009; 251:13–22. [PubMed: 19332842]
17. Feinendegen LE. Evidence for beneficial low level radiation effects and radiation hormesis. *Br J Radiol*. 2005; 78:3–7. [PubMed: 15673519]
18. Brenner DJ, Doll R, Goodhead DT, et al. Cancer risks attributable to low doses of ionizing radiation: assessing what we really know. *Proc Natl Acad Sci U S A*. 2003; 100:13761–13766. [PubMed: 14610281]
19. Pearce MS, Salotti JA, Little MP, et al. Radiation exposure from CT scans in childhood and subsequent risk of leukaemia and brain tumours: a retrospective cohort study. *Lancet*. 2012; 380:499–505. [PubMed: 22681860]
20. Mathews JD, Forsythe AV, Brady Z, et al. Cancer risk in 680,000 people exposed to computed tomography scans in childhood or adolescence: data linkage study of 11 million Australians. *Br Med J*. 2013; 346:f2360. [PubMed: 23694687]
21. Sedelnikova OA, Rogakou EP, Panyutin IG, et al. Quantitative detection of (125) IdU-induced DNA double-strand breaks with gamma-H2AX antibody. *Radiat Res*. 2002; 158:486–492. [PubMed: 12236816]
22. Rogakou EP, Pilch DR, Orr AH, et al. DNA double-stranded breaks induce histone H2AX phosphorylation on serine 139. *J Biol Chem*. 1998; 273:5858–5868. [PubMed: 9488723]
23. Rogakou EP, Boon C, Redon C, et al. Megabase chromatin domains involved in DNA double-strand breaks in vivo. *J Cell Biol*. 1999; 146:905–916. [PubMed: 10477747]
24. Pilch DR, Sedelnikova OA, Redon C, et al. Characteristics of gamma-H2AX foci at DNA double-strand breaks sites. *Biochem Cell Biol*. 2003; 81:123–129. [PubMed: 12897845]
25. Paull TT, Rogakou EP, Yamazaki V, et al. A critical role for histone H2AX in recruitment of repair factors to nuclear foci after DNA damage. *Curr Biol*. 2000; 10:886–895. [PubMed: 10959836]
26. Turner HC, Brenner DJ, Chen Y, et al. Adapting the gamma-H2AX assay for automated processing in human lymphocytes. 1. Technological aspects. *Radiat Res*. 2011; 175:282–290. [PubMed: 21388271]
27. Lobrich M, Rief N, Kuhne M, et al. In vivo formation and repair of DNA double-strand breaks after computed tomography examinations. *Proc Natl Acad Sci U S A*. 2005; 102:8984–8989. [PubMed: 15956203]
28. Redon CE, Nakamura AJ, Gouliava K, et al. The use of gamma-H2AX as a biodosimeter for total-body radiation exposure in non-human primates. *PLoS One*. 2010; 5:e15544. [PubMed: 21124906]
29. Beels L, Bacher K, De Wolf D, et al. gamma-H2AX foci as a biomarker for patient X-ray exposure in pediatric cardiac catheterization: are we underestimating radiation risks? *Circulation*. 2009; 120:1903–1909. [PubMed: 19858412]
30. Redon CE, Dickey JS, Bonner WM, et al. gamma-H2AX as a biomarker of DNA damage induced by ionizing radiation in human peripheral blood lymphocytes and artificial skin. *Adv Space Res*. 2009; 43:1171–1178. [PubMed: 20046946]
31. Stamm G, Nagel HD. CT-expo — a novel program for dose evaluation in CT. *Röfo*. 2002; 174:1570–1576. [PubMed: 12471531]
32. Valentin J. Basic anatomical and physiological data for use in radiological protection: reference values: a report of age- and gender-related differences in the anatomical and physiological

- characteristics of reference individuals. ICRP Publication 89. Ann ICRP. 2002; 32:5–265. [PubMed: 14506981]
33. Fenech M. The in vitro micronucleus technique. *Mutat Res.* 2000; 455:81–95. [PubMed: 11113469]
  34. Angelini S, Kumar R, Carbone F, et al. Micronuclei in humans induced by exposure to low level of ionizing radiation: influence of polymorphisms in DNA repair genes. *Mutat Res.* 2005; 570:105–117. [PubMed: 15680408]
  35. Andreassi MG, Ait-Ali L, Botto N, et al. Cardiac catheterization and long-term chromosomal damage in children with congenital heart disease. *Eur Heart J.* 2006; 27:2703–2708. [PubMed: 16717079]
  36. Bauchinger M. Quantification of low-level radiation exposure by conventional chromosome aberration analysis. *Mutat Res.* 1995; 339:177–189. [PubMed: 7491126]
  37. Rothkamm K, Balroop S, Shekhdar J, et al. Leukocyte DNA damage after multi-detector row CT: a quantitative biomarker of low-level radiation exposure. *Radiology.* 2007; 242:244–251. [PubMed: 17185671]
  38. Beels L, Bacher K, Smeets P, et al. Dose-length product of scanners correlates with DNA damage in patients undergoing contrast CT. *Eur J Radiol.* 2012; 81:1495–1499. [PubMed: 21596504]
  39. Schlattl H, Zankl M, Becker J, et al. Dose conversion coefficients for paediatric CT examinations with automatic tube current modulation. *Phys Med Biol.* 2012; 57:6309–6326. [PubMed: 22990300]
  40. Brix G, Lechel U, Veit R, et al. Assessment of a theoretical formalism for dose estimation in CT: an anthropomorphic phantom study. *Eur Radiol.* 2004; 14:1275–1284. [PubMed: 15034744]
  41. Jost G, Golfier S, Pietsch H, et al. The influence of x-ray contrast agents in computed tomography on the induction of dicentric and gamma-H2AX foci in lymphocytes of human blood samples. *Phys Med Biol.* 2009; 54:6029–6039. [PubMed: 19779223]
  42. Paterson A, Frush DP, Donnelly LF. Helical CT of the body: are settings adjusted for pediatric patients? *AJR Am J Roentgenol.* 2001; 176:297–301. [PubMed: 11159060]
  43. Picano E. Sustainability of medical imaging. *Br Med J.* 2004; 328:578–580. [PubMed: 15001510]
  44. Commission, E. Radiation protection 118 — referral guideline for imaging. Luxembourg: Office for Official Publications of the European Communities; 2001.

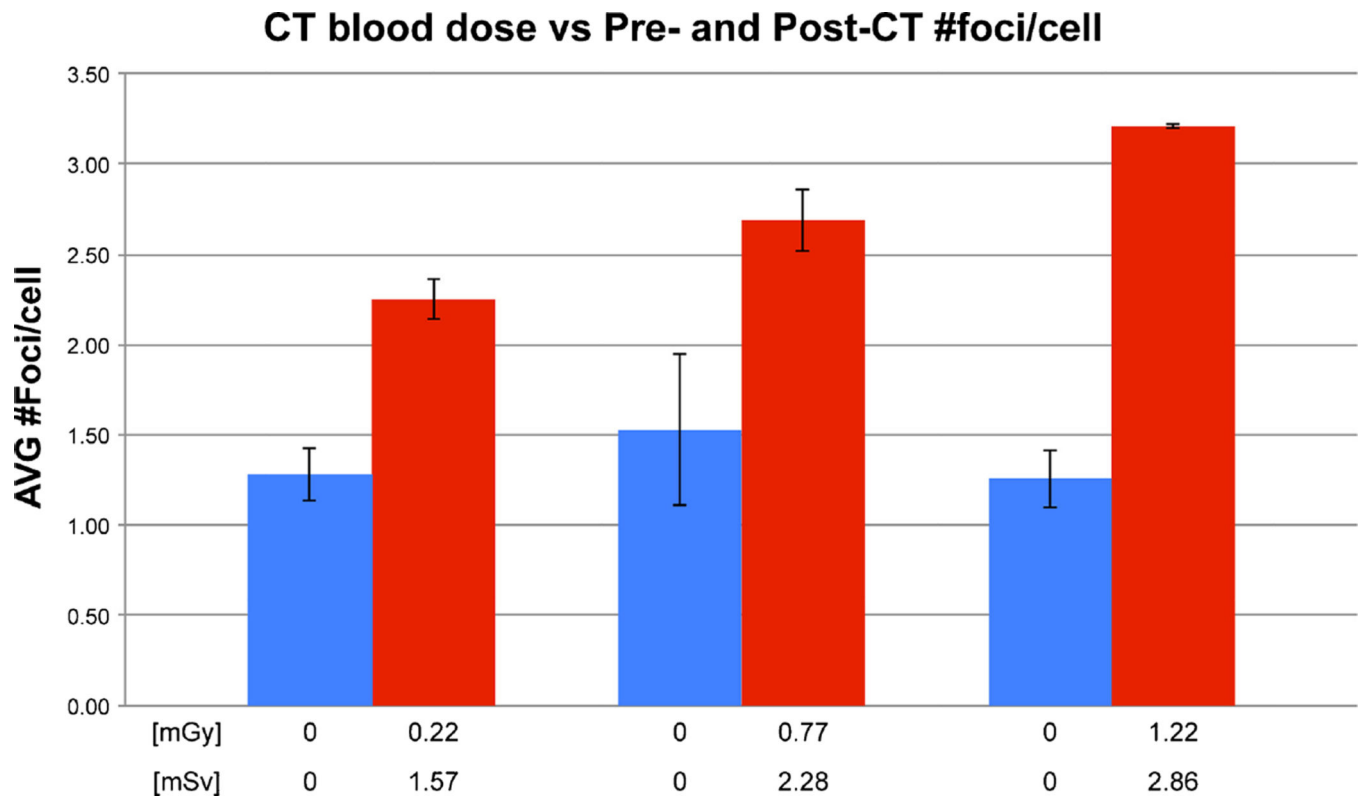


**Fig. 1.** Post-CT (*red bars*) versus pre-CT (*blue bars*) changes in lymphocytic  $\gamma$ -H2AX foci from three young children as a function of CT-induced ionizing radiation dose (expressed in blood dose [mGy] and in effective dose [mSv]); the means of the average foci per cell are presented. Error bars represent standard deviations between means of blinded duplicate analyses

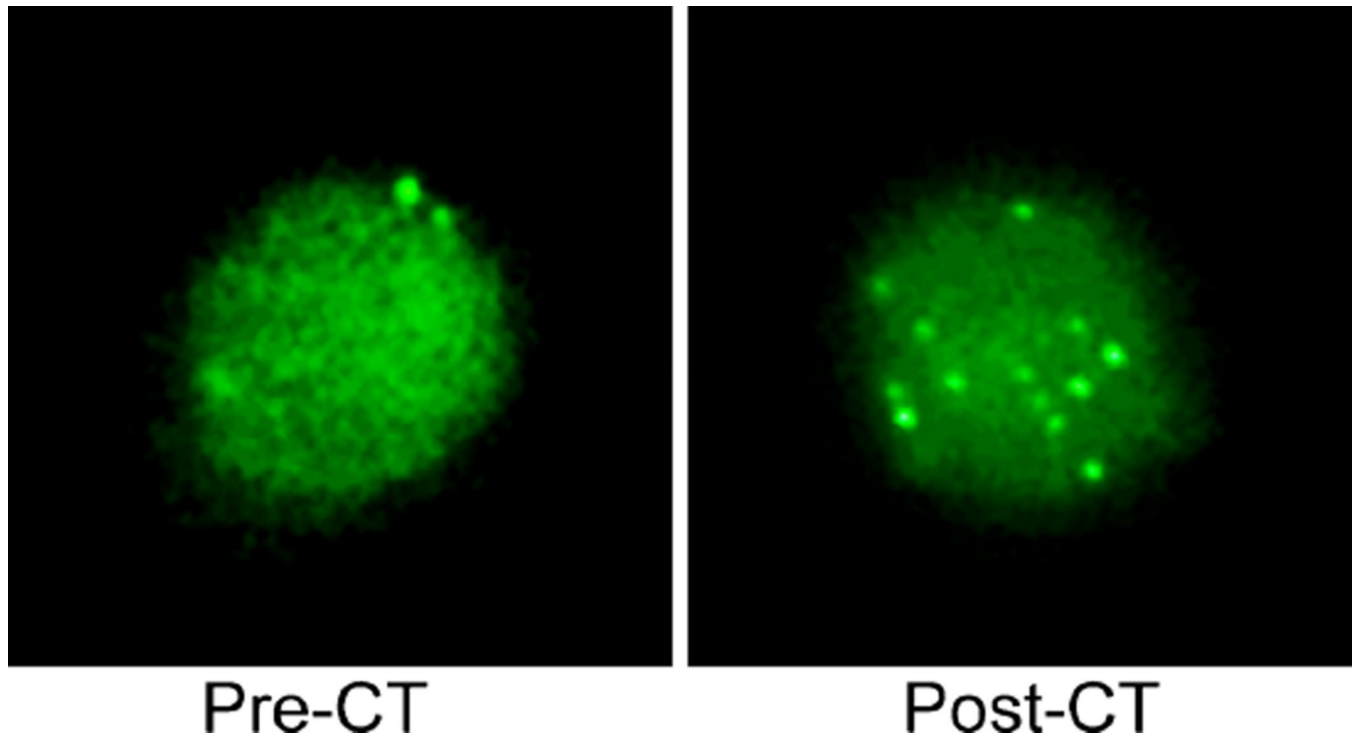


**Fig. 2.**  
Cell preparation with responses before and after CT (0.77 mGy blood dose) in a 15-month-old boy. Mean responses are shown in Fig. 1

Table 1

Calculations of total blood doses

Tissue or organ	Blood fraction in tissue or organ <sup>a</sup>	H <sub>T</sub> <sup>b</sup> per series for patient 1	H <sub>T</sub> <sup>b</sup> per series for patient 2	H <sub>T</sub> <sup>b</sup> per series for patient 3	Blood dose		
					Weighted organ doses for patient 1 <sup>c</sup>	Weighted organ doses for patient 2 <sup>c</sup>	Weighted organ doses for patient 3 <sup>c</sup>
Thyroid	0.001	7.1	1.1	3.1	0.004	0.002	0.001
Esophagus	0.010	1.6	0.3	1.1	0.016	0.011	0.003
Lungs	0.105	0.5	0.2	0.6	0.048	0.063	0.026
Liver	0.100	0.1	0.1	0.2	0.009	0.015	0.005
Stomach	0.010	0.1	0.0	0.1	0.001	0.001	0.000
Bone marrow	0.040	1.4	4.0	8.8	0.057	0.350	0.160
Bone surface	0.008	5.0	19.0	35.8	0.040	0.287	0.152
Skin	0.030	1.1	2.7	5.3	0.032	0.158	0.082
Brain	0.012	0.8	28.4	27.4	0.010	0.329	0.341
Spleen	0.014	0.1	0.0	0.1	0.001	0.002	0.001
Pancreas	0.006	0.1	0.0	0.1	0.000	0.001	0.000
Kidneys	0.020	0.0	0.0	0.1	0.001	0.001	0.000
				Total blood dose [mGy]	0.218	1.220	0.771

<sup>a</sup> Obtained from International Commission on Radiological Protection (ICRP) Publication 89, Section 7.7.2 p 142 [32]<sup>b</sup> H<sub>T</sub> = Organ dose (mSv). Calculated using software CT-Expo and based on conversion coefficient for standard patients ("Child" or "Baby")—see Materials and methods<sup>c</sup> Weighted organ dose = Blood fraction in tissue or organ \* Organ dose (mSv)

Table 2

Demographics and ionizing radiation dose of study participants

Patient ID	Age (mo)	Gender	Diagnosis	Radiation history	CT exam	DLP total exam dose (mGy-cm)	k conversation factors (mSv per mGy-cm)	Effective dose (mSv)	Organ dose (mGy) <sup>a</sup>	Total blood dose (mGy) <sup>b</sup>
1	3	male	neck abscess	2 CXR	neck w/contrast	92.46	0.017	1.57	21.9	0.22
2	21	male	macrocephaly	1 head CT, 1 CXR	head w/o contrast	426.12	0.0067	2.86	115.6	1.22
3	15	male	fever, seizure	none	head w/o contrast	340.89	0.0067	2.28	92.2	0.77

<sup>a</sup>Calculated using CT-Expo software (See Materials and methods)

<sup>b</sup>Total blood dose was calculated by multiplying the calculated organ dose by the fraction of the total blood volume present in each organ at any given time; the weighted organ doses were then summed to equal total blood dose (See Materials and methods)

CXR chest radiograph, *DLP* dose-length product